Journal of Sound and Vibration 325 (2009) 974–988

Contents lists available at ScienceDirect

Journal of Sound and Vibration

journal homepage: www.elsevier.com/locate/jsvi

Basic treatment of onset conditions and transient effects in thermoacoustic Stirling engines

A.T.A.M. de Waele *

Department of Applied Physics, Eindhoven University of Technology, Den Dolech 2, 5612 AZ Eindhoven, The Netherlands

ARTICLE INFO

Article history:
Received 22 August 2008
Received in revised form
28 March 2009
Accepted 30 March 2009
Handling Editor: C.L. Morfey
Available online 8 May 2009

ABSTRACT

This paper treats the basics of thermoacoustic engines. The set of differential equations, which describes the dynamics of the individual components, is condensed in a single high-order differential equation which determines the time dependence of all dynamic variables. From this relation analytical expressions are obtained for the damping coefficient, the oscillation frequency, and the onset temperature that allows stable oscillations. Also transient effects are discussed based on numerical integration of the dynamic equations.

1. Introduction

This paper treats the basics of thermoacoustic engines. The formalism that is presented here is general and can be applied to a large variety of thermal engines. The basic idea is that the set of differential equations, which describes the dynamics of the individual components, is condensed in a single high-order differential equation which is the heart of the dynamics of the entire system. It determines the time dependence of all dynamic variables. The so-called travelling-wave thermoacoustic Stirling engine, described in the paper by Backhaus and Swift [1], will be taken as the model system. This is a very important type of thermoacoustic engine which is studied in many laboratories around the world. Fig. 1 is a schematic drawing of this engine. It consists of a long resonator tube and a loop which contains a regenerator, several heat exchangers, a compliance (c), a connecting tube (d), a pulse tube (t), and a section, with a smaller diameter, called the inertance. One of the characteristic features of this engine is that the gas starts to oscillate back and forth in the machine "spontaneously" if the middle heat exchanger, with temperature T_t, is heated to a temperature which is sufficiently high above ambient temperature T_a. This effect is the main topic of this paper.

After explaining the model, the various differential equations will be derived, taking the temperature T_t as a fixed input parameter. This results in a single differential equation for the pressure p_t in the pulse tube. It will turn out to be a fourth-order differential equation with real constants. It will subsequently be solved analytically and its properties will be discussed. Expressions for the damping coefficient and conditions for the onset and stability of oscillations are derived as well as the relations for the oscillation frequency. In the second part of the paper the heating power $\dot{Q}_t$ is fixed and T_t is treated as a slowly varying function of time. For this case the dynamic equations are solved numerically. It reveals that the state of steady oscillations is reached after an interesting transient period which may show bursts of high-amplitude oscillations. So far this effect has been poorly investigated experimentally. In the state of steady oscillations the results of the analytical treatment and the numerical calculations are in excellent agreement.

* Tel.: +31 40 247 4215; fax: +31 40 243 8272.
E-mail address: a.t.a.m.d.waele@tue.nl

0022-460X/$ - see front matter © 2009 Elsevier Ltd. All rights reserved.
doi:10.1016/j.jsv.2009.03.043

Nomenclature

a	notation (Eqs. (9), (38)–(41))
a, b, c, f, k, l, m, n	notations (Eqs. (58) and (59))
A	area (m^2)
c	velocity of sound (m/s)
c_i	dimensionless parameters (Eq. (75))
C	flow conductance (m^3/Pa)
C_H	heat capacity of heat exchanger (J/K)
D	diameter (m)
f	volume rate of change (m^3/s)
$\overset{*}{H}$	enthalpy flow rate (W)
L	length (m)
M	mass (kg)
p	pressure (Pa)
$\dot{Q}$	heating power (W)
s	rate parameter (Eq. (42)) (s^{-2})
t	time (s)
T	temperature (K)
v	velocity (m/s)
V	volume (m^3)
$\overset{*}{V}$	volume flow rate (m^3/s)
w	compliance factor (m^3/Pa)
x	position (m), dimensionless time
z_r	specific flow impedance (m^{-2})
z	mathematical parameter
Z_r	geometrical flow impedance of the regenerator (Eq. (27)) (m^{-3})

Greek symbols

α	dimensionless damping parameter
γ	specific heat ratio
η	viscosity (sPa)
κ_a	effective thermal conductivity (W/Km)
ν	frequency (Hz)
τ	dimensionless temperature
ω	angular frequency (rad/s)
ω_x	dimensionless angular frequency

Subscripts

0	time average, characteristic
a	ambient
ac	acoustic
c	critical
c, d, f, R, t	spaces in the system
e	effective
o	orifice
p	(time) period
r	regenerator, resonance
ref	reference value

2. Modeling

The dimensions of the components in the loop are all sufficiently smaller than the wavelength of the oscillations so it can be modeled as in Fig. 2. The loop is decomposed in compartments c, t, and d (in which the pressures are homogeneous), an inertance, and a regenerator. The inertance is supposed to behave as a solid piston with a mass M_i equal to the mass of the gas contained in the inertance part. The orifice, together with the buffer volume b, represent a load. We assume that there is dissipation only in the orifice and in the regenerator.

All volume flows in the loop can be determined from the local pressure and its time derivative except the volume flow $\overset{*}{V}_R$. The resonator is so long that there are fundamental delays in it due to the finite velocity of sound. It is a challenge for future analysis to model the resonator tube in acoustic terms. In this paper the resonator will be modeled as a cylinder with volume V_R (average length L_{R0} and cross sectional area A_R) of a space R, closed at the right by a piston with mass M_R. By modeling the system in this way we really discuss a kind of free-piston Stirling engine. It is assumed that the pressure

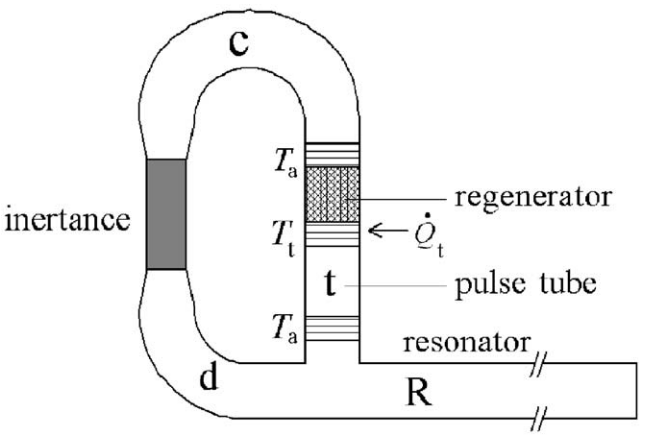

Fig. 1. Schematic drawing the travelling-wave thermoacoustic Stirling engine. The symbols are explained in the text.

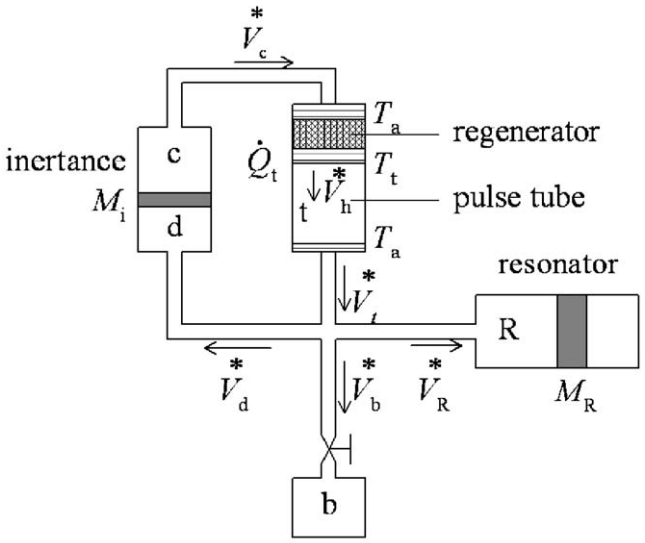

Fig. 2. Schematic drawing of the thermoacoustic engine. Compared to Fig. 1 the resonator tube is replaced by a volume V_R, closed by a piston with mass M_R. An orifice with flow conductance C_o, backed by a buffer volume b (which is assumed to be very large), is included to take into account dissipation in the system outside the regenerator.

inside V_R is only a function of time. The value of M_R is taken equal to the mass of the gas in V_R, so $M_R = \rho_0 L_{R0} A_R$ with ρ_0 the average density of the gas. The lower index 0 is used to indicate time-averaged values. The resonance frequency ω_R of the mass-gas-spring system formed by M_R and V_R is

$$\omega_R^2 = \frac{\gamma p_0}{\rho_0 L_{R0}^2}. \tag{1}$$

The basic angular resonance frequency ω_{ac} for an "open" tube (quarter wavelength), as in the case of Ref. [1], is given by

$$\frac{\omega_{ac} L_{ac}}{c} = \frac{1}{2}\pi \tag{2}$$

with c the velocity of sound. If we take the average length L_{R0} of the cylinder in such a way that $\omega_R = \omega_{ac}$ we have, using $\rho_0 c^2 = \gamma p_0$,

$$L_{R0} = \frac{2}{\pi} L_{ac}. \tag{3}$$

3. Dynamic equations

3.1. Governing equations

The properties of the resonator get index R and of the inertance index i. The pressures in the spaces t, d, and R are all equal to the pressure p_t in the pulse tube t. The pressure in c is p_c. The equation of motion of the mass of the inertance is

$$M_i \frac{d^2 x_i}{dt^2} = A_i (p_t - p_c) \tag{4}$$

with x_i the position of the mass M_i, counted positive in the upward direction. The volume of the space below M_i (space d) is given by

$$V_d = V_{d0} + A_i x_i. \tag{5}$$

With Eq. (5) relation (4) can be written in terms of the volume V_d

$$\frac{d^2 V_d}{dt^2} = \frac{A_i^2}{M_i} p_r, \tag{6}$$

where we wrote p_r for the pressure drop over the regenerator (and over the inertance)

$$p_r = p_t - p_c. \tag{7}$$

We will also use the notations

$$\delta p_t = p_t - p_0 \tag{8}$$

and

$$a_R = \frac{A_R^2}{M_R} \quad \text{and} \quad a_i = \frac{A_i^2}{M_i} \tag{9}$$

for convenience.

The acceleration of the mass M_R of the resonator is given by

$$M_R \frac{\mathrm{d}^2 x_R}{\mathrm{d}t^2} = A_R \delta p_t. \tag{10}$$

Since

$$V_R = V_{R0} + A_R x_R \tag{11}$$

we have

$$\frac{\mathrm{d}^2 V_R}{\mathrm{d}t^2} = a_R \delta p_t. \tag{12}$$

The volume flow through the orifice is given by

$$\overset{*}{V}_b = C_o \delta p_t, \tag{13}$$

with C_o the flow conductance of the orifice.

In Fig. 3 three situations are depicted: one where gas flows into and out of a control volume with volume V and pressure $p(t)$, one where gas flows into a control volume with a moving piston, and one where gas flows out of a container through a valve with flow conductance C. For these three situations we have three analogous relations. For the case of Fig. 3a

$$\overset{*}{V}_1 = \overset{*}{V}_2 + \frac{V}{\gamma p}\frac{\mathrm{d}p}{\mathrm{d}t}. \tag{14}$$

The nice thing about Eq. (14) is that it holds for an adiabatic ideal gas in the container, even if the temperature is not homogeneous. It holds, in particular, for the pulse tube where the temperature on one side is T_t and on the other side T_a.

For the case of Fig. 3b holds

$$\overset{*}{V}_1 = vA + \frac{V}{\gamma p}\frac{\mathrm{d}p}{\mathrm{d}t} \tag{15}$$

and for the case of Fig. 3c

$$0 = C(p - p_0) + \frac{V}{\gamma p}\frac{\mathrm{d}p}{\mathrm{d}t}. \tag{16}$$

In the analysis it will be assumed that the pressure variations are much smaller than the average pressure. In that case $V/\gamma p$ can be replaced by their average values $V_0/\gamma p_0$. Each of the spaces R, c, d, and t in the system of Fig. 2 can be characterized by the parameters

$$w_i = \frac{\gamma p_0}{V_{i0}} \quad \text{with } i = R, c, d, t. \tag{17}$$

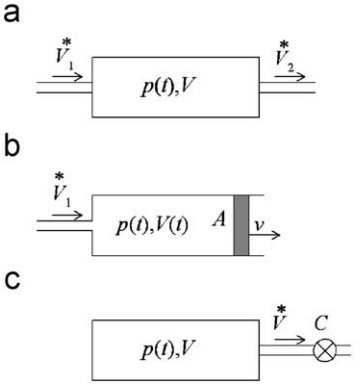

Fig. 3. Gas flows with varying pressure: (a) inlet and outlet; (b) inlet and piston; and (c) fixed volume with valve with flow conductance C.

With Eqs. (14)–(16) we can express the various volume flows, as defined in Fig. 2. With Eq. (14), applied to the pulse tube t,

$$\overset{*}{V}_h = \overset{*}{V}_t + \frac{1}{w_t}\frac{\mathrm{d}p_t}{\mathrm{d}t}. \tag{18}$$

With Eq. (15) and (5), applied to volume d,

$$\overset{*}{V}_d = \frac{\mathrm{d}V_d}{\mathrm{d}t} + \frac{1}{w_d}\frac{\mathrm{d}p_t}{\mathrm{d}t} \tag{19}$$

and, using Eq. (11) for R,

$$\overset{*}{V}_R = \frac{\mathrm{d}V_R}{\mathrm{d}t} + \frac{1}{w_R}\frac{\mathrm{d}p_t}{\mathrm{d}t} \tag{20}$$

and also for c

$$\overset{*}{V}_c = \frac{\mathrm{d}V_d}{\mathrm{d}t} - \frac{1}{w_c}\frac{\mathrm{d}p_c}{\mathrm{d}t}. \tag{21}$$

Mass conservation gives

$$\overset{*}{V}_t = \overset{*}{V}_b + \overset{*}{V}_d + \overset{*}{V}_R. \tag{22}$$

For simplicity we assume that the void volume in the regenerator is zero (zero compliance). In that case mass conservation over the regenerator gives

$$\overset{*}{V}_h = \tau_t \overset{*}{V}_c \tag{23}$$

with the reduced hot-end temperature

$$\tau_t = \frac{T_t}{T_a}. \tag{24}$$

In a linear approximation the volume flow, entering the regenerator, is proportional to the pressure drop p_R and can be written as

$$\overset{*}{V}_c = -C_r p_r. \tag{25}$$

The flow conductance C_r is written as

$$C_r = \frac{1}{\eta_a Z_r} \tag{26}$$

with η_a the viscosity at room temperature and

$$Z_r = \frac{z_r L_r}{A_r}, \tag{27}$$

where z_r is the specific flow resistance of the regenerator and L_r and A_r are the length and cross sectional area of the regenerator, respectively. In general C_r depends on the temperature distribution, etc. in the regenerator. More elaborate treatments of the regenerator can be found in Refs. [1,2]. For more detailed treatments numerical models can be used such as Sage [3], Regen3.2 [4], or DeltaE [5].

3.2. One dynamic equation

In the previous section the dynamic equations are given for each of the components of the engine. In this section these relations will be combined to the extreme, resulting in a single differential equation for one parameter (in fact δp_t) which determines the over-all dynamic behavior. The procedure is to eliminate subsequently all but one variable.

The volume flow $\overset{*}{V}_h$ in Eq. (18) can be eliminated with Eq. (23)

$$\tau_t \overset{*}{V}_c = \overset{*}{V}_t + \frac{1}{w_t}\frac{\mathrm{d}\delta p_t}{\mathrm{d}t} \tag{28}$$

and, with Eq. (25), $\overset{*}{V}_c$ can be eliminated

$$\tau_t C_r (p_c - p_t) = \overset{*}{V}_t + \frac{1}{w_t}\frac{\mathrm{d}\delta p_t}{\mathrm{d}t}. \tag{29}$$

Eqs. (13), (19), (20), and (29) in (22) give

$$\tau_t C_r p_r + \nu_t \frac{\mathrm{d}\delta p_t}{\mathrm{d}t} + C_o \delta p_t + \frac{\mathrm{d}V_d}{\mathrm{d}t} + \frac{1}{w_d}\frac{\mathrm{d}\delta p_t}{\mathrm{d}t} + \frac{\mathrm{d}V_R}{\mathrm{d}t} + \frac{1}{w_R}\frac{\mathrm{d}\delta p_t}{\mathrm{d}t} = 0. \tag{30}$$

With the notation

$$w_e = \frac{\gamma p_0}{V_t + V_{d0} + V_{R0}} \tag{31}$$

we get from Eq. (30)

$$-\frac{\mathrm{d}\delta p_t}{\mathrm{d}t} = \tau_t w_e C_r p_r + w_e C_o \delta p_t + w_e \frac{\mathrm{d}V_d}{\mathrm{d}t} + w_e \frac{\mathrm{d}V_r}{\mathrm{d}t}. \tag{32}$$

Eqs. (21), (25), and (7) give

$$C_r p_r = -\frac{\mathrm{d}V_d}{\mathrm{d}t} + \frac{1}{w_c}\frac{\mathrm{d}\delta p_t}{\mathrm{d}t} - \frac{1}{w_c}\frac{\mathrm{d}p_R}{\mathrm{d}t}. \tag{33}$$

With Eq. (32)

$$-\frac{\mathrm{d}p_r}{\mathrm{d}t} = (w_c + w_e)\frac{\mathrm{d}V_d}{\mathrm{d}t} + (\tau_t w_e C_r + w_c C_r)p_r + w_e C_o \delta p_t + w_e \frac{\mathrm{d}V_R}{\mathrm{d}t}. \tag{34}$$

We eliminate V_R and V_d by differentiating Eqs. (34) and (32) once. Substitution of Eq. (6) and (12) gives

$$-w_e C_o \frac{\mathrm{d}\delta p_t}{\mathrm{d}t} - w_e a_R \delta p_t = \frac{\mathrm{d}^2 p_r}{\mathrm{d}t^2} + (\tau_t w_e + w_c)C_r \frac{\mathrm{d}p_r}{\mathrm{d}t} + (w_c + w_e)a_i p_r \tag{35}$$

and

$$\frac{\mathrm{d}^2 \delta p_t}{\mathrm{d}t^2} + w_e C_o \frac{\mathrm{d}\delta p_t}{\mathrm{d}t} + w_e a_R \delta p_t = -\tau_t w_e C_r \frac{\mathrm{d}p_r}{\mathrm{d}t} - w_e a_i p_r. \tag{36}$$

Eqs. (35) and (36) form a set of two linear second-order differential equations with δp_t and p_r as variables. In Appendix A it is shown that elimination of p_r leads to a single homogeneous fourth-order differential equation in δp_t

$$\frac{\mathrm{d}^4 \delta p_t}{\mathrm{d}t^4} + a_3 \frac{\mathrm{d}^3 \delta p_t}{\mathrm{d}t^3} + a_2 \frac{\mathrm{d}^2 \delta p_t}{\mathrm{d}t^2} + a_1 \frac{\mathrm{d}\delta p_t}{\mathrm{d}t} + a_0 \delta p_t = 0 \tag{37}$$

with

$$a_3 = w_e C_o + w_c C_r + \tau_t w_e C_r, \tag{38}$$

$$a_2 = a_R w_e + a_i w_c + a_i w_e + w_c w_e C_r C_o, \tag{39}$$

$$a_1 = w_c w_e (C_r a_R + C_o a_i), \tag{40}$$

$$a_0 = w_c w_e a_R a_i. \tag{41}$$

Note that all factors are positive and that only a_3 depends on the dimensionless temperature τ_t.

3.3. Stable oscillations

Eq. (37) generally results in solutions which are oscillating in time. This is shown in more detail in Appendix A. The function s, defined in Eq. (84) as

$$s = \frac{a_1}{a_3} + a_0 \frac{a_3}{a_1} - a_2, \tag{42}$$

determines the growth or decay of oscillations. As shown in Appendix A the function s is proportional to the damping coefficient α with a positive proportionality constant. If $s>0$ the oscillations grow, if $s<0$ the oscillations are damped. In any case $s<0$ if $\tau_t = 1$, so the oscillations are always damped in an isothermal system (as it should).

For steady oscillations $s = 0$ so

$$0 = a_0 \left(\frac{a_3}{a_1}\right)^2 - a_2 \frac{a_3}{a_1} + 1 \tag{43}$$

or

$$\frac{a_3}{a_1} = \frac{a_2 \pm \sqrt{a_2^2 - 4a_0}}{2a_0} \tag{44}$$

and also (Eq. (86))

$$\omega^2 = \frac{a_1}{a_3}. \tag{45}$$

So the oscillation frequency is given by

$$\nu = \frac{1}{2\pi}\sqrt{\frac{a_1}{a_3}}. \tag{46}$$

In Eq. (44) only the solution with the minus sign gives a positive dimensionless temperature τ_t. Substitution of Eqs. (38)–(41) in Eq. (44) gives the relation for the temperature T_c at which the oscillations are stable

$$\frac{T_c}{T_a} = \tau_c = \frac{1}{2w_e}\left(\frac{1}{a_i} + \frac{C_o}{C_r a_R}\right)(a_2 + \sqrt{a_2^2 - 4a_0}) - \frac{C_o}{C_r} - \frac{w_c}{w_e}. \tag{47}$$

If the system is originally at room temperature and a sufficiently large heating power is applied, the oscillations start if the temperature has reached the critical value of T_c. Therefore this temperature will be called the onset temperature. Substituting τ_c in Eq. (38) and (45) gives the angular frequency of the oscillations.

Substituting Eqs. (39) and (41) in Eqs. (47) and (38) and (40) in Eq. (46) leads to rather complicated expressions which show how the various system parameters affect the onset temperature and the oscillation frequency. If $C_o = 0$ (no dissipation outside the regenerator) τ_c is given by

$$\tau_c = \frac{a_2 + \sqrt{a_2^2 - 4a_0} - 2w_c a_i}{2w_e a_i} \quad \text{if } C_o = 0. \tag{48}$$

It is independent of the regenerator conductance C_r. This somewhat surprising result is due to the fact that, on one hand, the flow in the regenerator gives dissipation, but, on the other hand, the pressure difference over the regenerator is the driving force for the oscillations. In the limit of small w_e (or large V_{R0}) and with $C_o = 0$ a second-order series expansion of the numerator in w_e shows that the onset temperature is given by

$$\frac{T_c}{T_a} = 1 + \frac{w_e a_R}{w_c a_i} \tag{49}$$

and the corresponding frequency by

$$\omega^2 = w_e a_R = \omega_{eR}^2. \tag{50}$$

So, in this limiting case, the system oscillates at the resonance frequency of the resonator tube. With the values of Table 3 Eq. (49) would lead to values of τ_c close to one while in practice τ_c is more on the order of two. This shows that, in reality, dissipation in the external circuit cannot be neglected ($C_o \neq 0$).

Table 1
Numerical values of the model system.

System parameter	Symbol	Value
Resonator diameter	D_R	0.102 m
Length ac resonator	L_{ac}	2 m
Regenerator diameter	D_r	0.0889 m
Length of regenerator	L_r	0.073 m
Specific impedance	z_r	3.6×10^9 m^{-2}
Length of pulse tube	L_t	0.24 m
Diameter of pulse tube	D_t	0.078 m
Average length of space d	L_{d0}	0.209 m
Diameter of space d	D_d	0.085 m
Length of inertance tube	L_i	0.256 m
Diameter of inertance tube	D_i	0.078 m
Average volume of space c	V_{c0}	0.00283 m^3
Ambient temperature	T_a	300 K
Average pressure	p_0	3 MPa
Specific-heat ratio	γ	1.67
Viscosity at T_a	η_a	20 μs Pa
Density	ρ_0	4.81 kg/m^3
Conductance orifice	C_o	$0.1C_r$

4. Some characteristic dependences

4.1. Input parameters

In this section some examples of calculated results will be given which show what can be done with the results obtained so far. It is not the purpose of this section to give an exhaustive treatment of all implications of the formulae given above. Unfortunately Ref. [1] does not give enough detailed information to make a quantitative comparison between the results, derived in this paper, and the actual performance of the system. The numerical values of our model system are given in Table 1. They are the same as the system described in Ref. [1].

4.2. Some plots

Next some plots are given for τ_c and the scaled oscillation frequency ν/ν_{ref} with $\nu_{\mathrm{ref}} = \omega_{\mathrm{eR}}/2\pi$. They are plotted as functions of C_o/C_r, D_i, and L_{ac} while the other system parameters have fixed values given in Table 1. In Fig. 4 the conductance C_o of the orifice is varied. We see that an onset temperature above ambient is necessary ($\tau_c > 1$) even if $C_o = 0$.

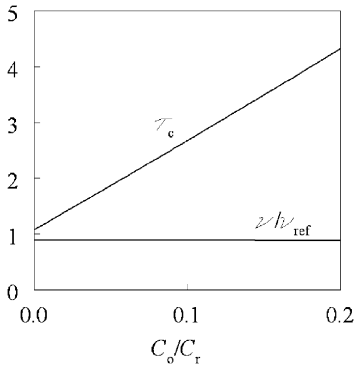

Fig. 4. Onset reduced temperature τ_c and scaled oscillation frequency ν/ν_{ref} as functions of the relative orifice conductance.

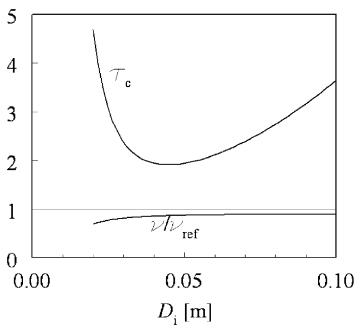

Fig. 5. Onset reduced temperature τ_c and scaled oscillation frequency ν/ν_{ref} as functions of the inertance diameter D_i.

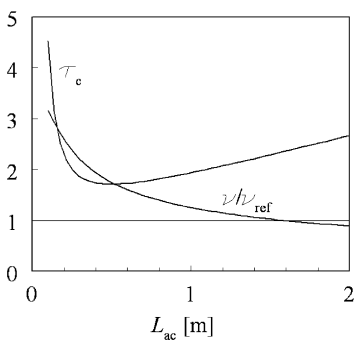

Fig. 6. Onset reduced temperature τ_c and scaled oscillation frequency ν/ν_{ref} as functions of the resonator length L_{ac}.

For stable oscillations a higher temperature is needed if the orifice conductance is increased. The oscillation frequency does not depend strongly on the orifice setting.

Fig. 5 is a plot with the inertance diameter D_i as variable. This plot shows a clear minimum of τ_c for $D_i = 4.5$ cm. Fig. 6 is a plot of the onset temperature and the reduced oscillation frequency as functions of L_{ac}. In this case there is a clear minimum of τ_c at $L_{ac} = 0.2$ m.

5. Transient behavior

So far T_t has been treated as an input parameter which is constant in time. We have seen that $T_t < T_c$ corresponds with $\alpha < 0$, so oscillations tend to die out. On the other hand $T_t > T_c$ corresponds with $\alpha > 0$. In this case the oscillations would grow without limitation if T_t is fixed. Hence also the heat flow $\dot{Q}_t$, needed to fix T_t, also would grow without limitation. It is more realistic to fix the heat flow $\dot{Q}_t$. This case will be considered in this section.

In the presence of an oscillating gas flow in the engine the temperature T_t oscillates with the same frequency. However, at frequencies in the acoustic region, the amplitude of the oscillations in the temperature of the heat exchanger is very small due to its high heat capacity C_h. If only slow temperature variations are considered, the energy balance of the heat exchanger is given by

$$C_H \frac{dT_t}{dt} = \dot{Q}_t - \dot{Q}_c - \overline{\overset{*}{H}_t}. \tag{51}$$

Here $\dot{Q}_t$ the applied heating power and $\dot{Q}_c$ the heat flow conducted to the surroundings. If the only path of the heat flow is through the regenerator then

$$\dot{Q}_c = \kappa_a \frac{A_r}{L_r}(T_t - T_a) \tag{52}$$

with κ_a the effective thermal conductivity of the regenerator. The average enthalpy flow in the pulse tube is taken over one oscillation period so we write

$$\overline{\overset{*}{H}_t} = \frac{1}{t_p}\int_t^{t+t_p} \overset{*}{V}_h \delta p_t \, dt, \tag{53}$$

where $t_p = 1/\nu$ is the time between two zero crossings of δp_t with a positive slope. Defined in this way, the average enthalpy flow is a short-time average which can vary slowly with time. The pressure amplitude p_1 is defined as the maximum value of δp_t during the time span t_p.

With

$$\frac{dV_d}{dt} = f_d \tag{54}$$

and

$$\frac{dV_R}{dt} = f_r. \tag{55}$$

Eqs. (6) and (12) result in

$$\frac{df_d}{dt} = a_i p_r \tag{56}$$

and

$$\frac{df_R}{dt} = a_R \delta p_t. \tag{57}$$

Eqs. (32), (34), (56), and (57) form a complete set of four first-order differential equations. The general solution of such a set is described in Ref. [6]. Here the set is solved numerically by second-order Runge–Kutta integration [7].

Fig. 7 gives the calculated time dependence of T_t and the amplitude of the pressure oscillations in the pulse tube p_1.[1] The value of the thermal conductance of the regenerator $\kappa_a A_r/L_r$ was set at 0.085 W/K. In order to speed up the effects the heat capacity C_H was given the rather low value of 0.21 J/K. For this system the onset temperature $T_c = \tau_c T_a = 802$ K. This is represented by a horizontal line in Fig. 7. With a thermal conductance of 0.085 W/K a critical heating power of 43 W is needed to maintain a temperature of 802 K. The applied heating power was $\dot{Q}_t = 500$ W, so far above the critical value. With this heating power the equilibrium temperature without oscillations (so with $\overline{\overset{*}{H}_t} = 0$) would be as high as 6182 K, so far above the onset temperature of 802 K.

Now let us have a look at Fig. 7. At $t = 0$ the initial temperature T_t was set at 600 K and δp_t was given a small kick of 50 hPa. As long as $T_t < 802$ K the temperature of the hot end is too low to sustain steady oscillations ($\alpha < 0$). The pressure

[1] In this discussion we will only mention p_1 as the amplitude of the oscillations, but it should be understood that the amplitudes of all other dynamic parameters, such as the pressure drop over the regenerator and the various volume flows, vary in the same way.

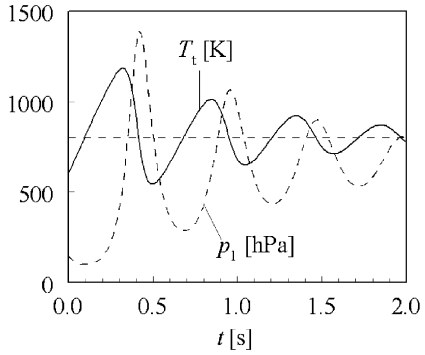

Fig. 7. Time dependences of T_t (full line) and p_1 (dotted line) for an artificially low C_H. The horizontal line represents the critical temperature.

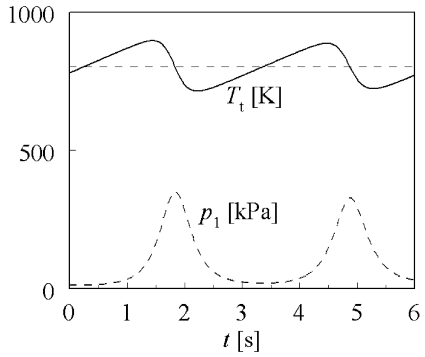

Fig. 8. Time dependences of T_t (full line) and p_1 (dotted line) for a realistic C_H. The horizontal line represents the critical temperature. The figure shows a repetition of bursts of high-intensity sound interrupted by relatively long quiet periods.

oscillations, resulting from the kick at the start, tend to die out. This is visible between $t = 0$ and 0.1 s. However, T_t increases rapidly and after about 0.1 second T_t reaches $T_c = 802$ K. From then on $T_t > T_c$ and the amplitude of the oscillations grows ($\alpha > 0$). This is associated with a rapid increase of the sound intensity illustrated in Fig. 7 by an increase of p_1. The frequency ν of the sound is about 103 Hz. Subsequently the hot end is cooled strongly by the oscillating gas flow (expressed in Eq. (51) by a high value of the average enthalpy flow) and, after going through a maximum, T_t decreases. But the amplitude of the sound keeps on growing as long as $T_t > T_c$. At the moment that the hot end has cooled to the onset temperature T_c the intensity of the oscillations is at its maximum! So T_t continues to drop to values below T_c, initially with a slow decay but later with a much stronger decay until the cooling of the hot heat exchanger by the oscillating gas becomes smaller than the applied heating power. From that moment the temperature T_t starts to move up again.

This is repeated with decreasing excursions until a state of steady oscillations is reached at $T_t = 802$ K. This value, obtained from the numerical integration, corresponds with $\tau_c = 2.67$ which is in excellent agreement with the value obtained from the analytical treatment (Eq. (47)). Also the numerically-obtained frequency ν of 102.9 Hz is equal to the value obtained by the analytical solution (45). In the steady state the enthalpy flow $\overline{\dot{H}_t^*} = 459$ W and the heat flow by conduction is $\dot{Q}_c = 41$ W.

The situation for $T_t \approx T_c$ can be understood as follows: if $T_t < T_c$ the oscillations are damped. Due to the applied heating power the temperature rises. At the moment T_t passes T_c the oscillations grow according to $\exp(\alpha t)$, but α grows linearly in time. So the oscillation amplitudes grow more than exponential. Setting $t = 0$ at the moment that $T_t = T_c$ the oscillations grow with $\exp(\alpha' t^2\, \mathrm{d}T_t/\mathrm{d}t)$ with α' a positive constant.

The repetition rate of bursts of acoustic power (with a frequency of about 2 Hz in the example of Fig. 7) is determined by the interplay between the heating power, the rate of the grow and decay of the amplitude of the high-frequency oscillations (sound intensity), and the heat capacity C_h of the region around the hot heat exchanger. At values of the heating power just above the critical value the repetition rate is small and increases with $\dot{Q}_t$.

Fig. 8 represents the calculated variations of T_t and p_1 as functions of time for the more realistic value of $C_H = 21$ J/K. The applied heating power was 2 kW and the starting temperature 750 K, so not too far below the critical temperature. The figure shows a repetition of bursts of very high intensity sound interrupted by relatively long quiet periods. Also in this case we see transient effects with a certain time period which is, in this case, about 3 s. The oscillation amplitudes of the pressure are strong functions of time and, in this example, can vary over an order of magnitude.

It is interesting to note that, under the conditions in this paper, the value of T_c is determined only by the geometry of the machine and not by the heating power $\dot{Q}_t$. Consequently, in the steady state, also the heat flow $\dot{Q}_c$ is independent of $\dot{Q}_t$. Only the oscillation amplitude p_1 is affected by $\dot{Q}_t$ and, consequently, the average enthalpy flow $\overline{\dot{H}_t^*}$. During the transient period, at the peak values of the p_1-oscillations, the energy flows are very high (in the example of Fig. 8 more than 12 kW), so large radial temperature gradients will be present heat exchanger. This will affect the dynamics of the behavior. Also the assumptions of linearity of the relations will not be valid at high amplitudes. It is an interesting situation that the onset of the oscillations is determined by the values of, e.g. C_R and C_o for small amplitudes, but that the effective values of these system parameters may differ for oscillations with high amplitudes.

The transient behavior, reported in this section, has been observed experimentally [9]. Penelet et al. have reported effects that strongly resemble the pulsating oscillations described here [10]. Penelet et al. conclude that their model does not reproduce the experimental results very well. They argue that the most critical assumption in the model is the one-dimensional approach in the description of the heat transfer. It would be interesting to reanalyze their system in terms of the model presented in this paper. Yu et al. used CFD software to calculate the transient behavior in their machine for two conditions: one with fixed heat input (case A) and one with fixed hot-end temperature (case B) [11]. Case A corresponds with the numerical approach in this paper (Section 5). They find an overshoot of the pressure amplitude before it tends to a state of steady oscillations. This is resembles the results found here. Case B of Yu et al. corresponds with the analytical treatment of this paper. In the treatment, given in Section 4, the amplitude would grow without limitation once the critical temperature is passed. This is in contrast with the findings of Yu et al. The reason is most probably that the dissipation strongly increases at high amplitudes, e.g. due to vortex production. This is favored by the geometry chosen by Yu et al. where the gas is forced to make a 180° angle. This kind of effects is not taken into account in this paper (although is can be incorporated in C_o). Furthermore heat exchange may become problematic if the gas oscillates with high amplitude so the condition of constant temperature is not satisfied. The combination of these effects would also explain that there is only a single small overshoot in Case A.

6. Discussion

In this paper the basic features of thermoacoustic engines are treated with the travelling-wave thermoacoustic heat engine as a working model. If the hot-end temperature is assumed to be constant the dynamics of the system is described by a fourth-order differential equation which determines damping, growth, or stability of oscillations. For the case that the hot-end temperature is allowed to vary in time the dynamic relations are integrated numerically. Interesting transient effects are seen in which the amplitude of the oscillations is pulsating. Eventually a steady state is reached in which the amplitudes of the oscillations are stable. The results of the numerical integration for the steady state agree very well with the analytical relations.

Acknowledgments

This work is partly supported by MicroNed, Project number 1-B-7. The interest of the team of the Low-Temperature group, in particular J.C.H. Zeegers and H.J.M. ter Brake, was very stimulating. S.W. Rienstra is acknowledged for useful suggestions. M.E.H. Tijani is acknowledged for his stimulating interest and critical reading of the manuscript.

Appendix A. Derivations

Eqs. (35) and (36) with the following identifications:

$$a=(\tau_t w_e+w_c)C_r,\quad b=(w_c+w_e)a_i,\quad c=-w_eC_o,\quad f=-a_Rw_e, \tag{58}$$

$$k=w_eC_o,\quad l=a_Rw_e,\quad m=-\tau_t w_eC_r,\quad n=-a_iw_e \tag{59}$$

become

$$\frac{\mathrm{d}^2p_r}{\mathrm{d}t^2}+a\frac{\mathrm{d}p_r}{\mathrm{d}t}+bp_r=c\frac{\mathrm{d}\delta p_t}{\mathrm{d}t}+f\delta p_t \tag{60}$$

and

$$\frac{\mathrm{d}^2\delta p_t}{\mathrm{d}t^2}+k\frac{\mathrm{d}\delta p_t}{\mathrm{d}t}+l\delta p_t=m\frac{\mathrm{d}p_r}{\mathrm{d}t}+np_r. \tag{61}$$

Multiplying Eq. (61) with the operator

$$O_a=\frac{\mathrm{d}^2}{\mathrm{d}t^2}+a\frac{\mathrm{d}}{\mathrm{d}t}+b \tag{62}$$

gives

$$\left(\frac{d^2}{dt^2}+a\frac{d}{dt}+b\right)\left(\frac{d^2\delta p_t}{dt^2}+k\frac{d\delta p_t}{dt}+l\delta p_t\right)=\left(\frac{d^2}{dt^2}+a\frac{d}{dt}+b\right)\left(m\frac{dp_r}{dt}+np_r\right) \tag{63}$$

or

$$\left(\frac{d^2}{dt^2}+a\frac{d}{dt}+b\right)\left(\frac{d^2\delta p_t}{dt^2}+k\frac{d\delta p_t}{dt}+l\delta p_t\right)=\left(m\frac{d}{dt}+n\right)\left(\frac{d^2p_r}{dt^2}+a\frac{dp_r}{dt}+bp_r\right). \tag{64}$$

With Eq. (60)

$$\left(\frac{d^2}{dt^2}+a\frac{d}{dt}+b\right)\left(\frac{d^2\delta p_t}{dt^2}+k\frac{d\delta p_t}{dt}+l\delta p_t\right)=\left(m\frac{d}{dt}+n\right)\left(c\frac{d\delta p_t}{dt}+f\delta p_t\right). \tag{65}$$

Expanding this relation and collecting terms gives

$$0=\frac{d^4\delta p_t}{dt^4}+a_3\frac{d^3\delta p_t}{dt^3}+a_2\frac{d^2\delta p_t}{dt^2}+a_1\frac{d\delta p_t}{dt}+a_0\delta p_t \tag{66}$$

with

$$a_3=k+a, \tag{67}$$

$$a_2=l+ak-cm+b, \tag{68}$$

$$a_1=al-fm-cn+bk, \tag{69}$$

$$a_0=bl-fn. \tag{70}$$

If we would eliminate δp_t instead of p_R we would have obtained the same differential equation but now in p_R. This reflects the fact that the stability condition for all dynamic variables is the same.

We write Eq. (66) as

$$0=\frac{d^4\delta p_t}{a_0dt^4}+\frac{a_3}{a_0}\frac{d^3\delta p_t}{dt^3}+\frac{a_2}{a_0}\frac{d^2\delta p_t}{dt^2}+\frac{a_1}{a_0}\frac{d\delta p_t}{dt}+\delta p_t. \tag{71}$$

This suggests a characteristic frequency

$$\omega_0=a_0^{1/4}. \tag{72}$$

We introduce the dimensionless time x according to

$$x=\omega_0 t \tag{73}$$

then Eq. (71) reduces to

$$0=\frac{d^4\delta p_t}{dx^4}+c_3\frac{d^3\delta p_t}{dx^3}+c_2\frac{d^2\delta p_t}{dx^2}+c_1\frac{d\delta p_t}{dx}+\delta p_t \tag{74}$$

with

$$c_3=\frac{a_3}{\omega_0},\quad c_2=\frac{a_2}{\omega_0^2},\quad c_1=\frac{a_1}{\omega_0^3}. \tag{75}$$

Note that all coefficients in Eq. (74) are real and positive. The solution of Eq. (74) is of the form [7]

$$\delta p_t=\sum_{k=1}^{4}C_k\exp(z_kx), \tag{76}$$

where the z_k are the roots of the characteristic equation

$$0=z^4+c_3z^3+c_2z^2+c_1z+1. \tag{77}$$

Eq. (76) is the general solution of the time dependence of δp_t for constant τ_t. It contains not only eventual oscillatory solutions, but also all transient effects such as the transition to a steady state after an arbitrary starting condition. Eventual oscillatory solutions are not a prerequisite of our treatment, but rather the result.

Eq. (77) can be solved analytically [8]. If one root is complex its complex conjugate is also a root since the coefficients c_1, c_2, and c_3 are real. In that case the linearly independent solutions are

$$e^{\alpha x}\cos\omega_x x\quad\text{and}\quad e^{\alpha x}\sin\omega_x x. \tag{78}$$

The index x in ω_x is used to indicate that ω_x is the angular frequency expressed in the dimensionless time x.

We substitute

$$z = \alpha + \mathrm{i}\omega_x \tag{79}$$

in Eq. (77). We are interested in the onset of oscillations, so we can limit the discussion to low values of α. To first order in α Eq. (77) gives

$$0 = -4\mathrm{i}\alpha\omega_x^3 - 3c_3\alpha\omega_x^2 + 2\mathrm{i}c_2\alpha\omega_x + c_1\alpha + \omega_x^4 - \mathrm{i}c_3\omega_x^3 - c_2\omega_x^2 + \mathrm{i}c_1\omega_x + 1. \tag{80}$$

The real part of Eq. (80) results in

$$0 = \omega_x^4 - (3c_3\alpha + c_2)\omega_x^2 + c_1\alpha + 1 \tag{81}$$

and the imaginary part in

$$\omega_x^2 = \frac{c_1}{c_3} + \alpha\left(2\frac{c_2}{c_3} - 4\frac{c_1}{c_3^2}\right). \tag{82}$$

Substituting Eq. (82) in (81) gives, with Eq. (75), to lowest order in α,

$$\alpha = \frac{1}{2}\frac{c_1c_3^2}{c_1c_3^3 + (2c_1 - c_2c_3)^2}\frac{1}{a_0^{1/2}}\left(\frac{a_1}{a_3} + a_0\frac{a_3}{a_1} - a_2\right). \tag{83}$$

As the prefactor is positive the sign of α is determined by the sign of the function

$$s = \frac{a_1}{a_3} + a_0\frac{a_3}{a_1} - a_2. \tag{84}$$

If $s<0$ the oscillations are damped. If $s>0$ the oscillation amplitude is growing.

For steady oscillations $s = 0$. In this case Eq. (82) gives

$$\omega_x^2 = \frac{c_1}{c_3}. \tag{85}$$

The real-time angular frequency is given by

$$\omega^2 = \omega_0^2\omega_x^2 = \frac{a_1}{a_3}. \tag{86}$$

With $\alpha = 0$ Eqs. (81) and (82) give

$$c_2 = \frac{c_1}{c_3} + \frac{c_3}{c_1}. \tag{87}$$

Substitution of Eq. (87) in Eq. (77) reads

$$0 = z^4 + c_3z^3 + \left(\frac{c_1}{c_3} + \frac{c_3}{c_1}\right)z^2 + c_1z + 1. \tag{88}$$

Eq. (88) can be written as

$$0 = \left(z^2 + \frac{c_1}{c_3}\right)\left(z^2 + c_3z + \frac{c_3}{c_1}\right). \tag{89}$$

The first factor gives the two roots

$$z_{1,2} = \pm\mathrm{i}\sqrt{\frac{c_1}{c_3}} \tag{90}$$

which we know from Eq. (85). The second set of roots $z_{3,4}$ is given by

$$z_{3,4} = \frac{1}{2}\left(-c_3 \pm \sqrt{c_3^2 - \frac{4c_3}{c_1}}\right). \tag{91}$$

As $c_3>0$ the second set of solutions $z_{3,4}$ corresponds with damped oscillations. So there is only one steady oscillation possible. The property differs from real thermoacoustic systems where higher harmonics are possible. This can be mimicked in our model by choosing different values for the parameter a_R.

Table 2 gives the calculated coefficients in the characteristic equations of the model system. The fact that the dimensionless parameters c_1, c_2, and c_3 are of order 1 is an indication that they are good dimensionless parameters to characterize the basic properties of the system.

Table 2
Coefficients in the characteristic equations of the model system.

Symbol	Expression	Value	Symbol	Value
a_0	71	$3.59 \times 10^{12}\ s^{-4}$	c_0	1
a_1	70	$1.41 \times 10^{9}\ s^{-3}$	c_1	0.54
a_2	69	$8.99 \times 10^{6}\ s^{-2}$	c_2	4.75
a_3	68	$3.37 \times 10^{3}\ s^{-1}$	c_3	2.45

Table 3
Characteristic frequencies for the model system defined in Table 1.

Symbol	Expression	Value (Hz)
ν_{Ccr}	$w_c C_R/2\pi$	332
ν_{Cer}	$w_e C_R/2\pi$	73.8
ν_{Ceo}	$w_e C_o/2\pi$	7.38
ν_{eR}	$\sqrt{a_R w_e}/2\pi$	115
ν_{ci}	$\sqrt{a_i w_c}/2\pi$	417
ν_{ei}	$\sqrt{a_i w_e}/2\pi$	196
ν	Eq. (47)	102.92

Appendix B. Characteristic frequencies

The combination of the compliance volume V_c and the regenerator conductance C_r, the volume V_e and C_r, and V_e and the orifice conductance C_o are all examples of case *c* of Fig. 2. The rate of change of the pressure in the vessel is determined by three characteristic frequencies

$$\omega_{Ccr} = w_c C_r, \tag{92}$$

$$\omega_{Cer} = w_e C_r, \tag{93}$$

$$\omega_{Ceo} = w_e C_o. \tag{94}$$

The product $w_e a_R$

$$\omega_{eR}^2 = a_R w_e = a_R \frac{\gamma p_0}{V_e} \tag{95}$$

is the square of the angular resonance frequency of the mass of the piston and the gas-spring action due to the volume V_e. Similarly

$$\omega_{ci}^2 = a_i w_c, \tag{96}$$

$$\omega_{ei}^2 = a_i w_e \tag{97}$$

are the resonance frequencies of the mass-spring systems formed by the inertance and the compliance and the inertance and V_e, respectively. Table 3 gives the values of the various frequencies for the model system.

With these frequencies Eqs. (35) and (36) become

$$\frac{d^2 p_r}{dt^2} + (\tau_t \omega_{Cer} + \omega_{Ccr}) \frac{dp_r}{dt} + (\omega_{ci}^2 + \omega_{ei}^2) p_r = -\omega_{Ceo} \frac{d\delta p_t}{dt} - \omega_{eR}^2 \delta p_t \tag{98}$$

and

$$\frac{d^2 \delta p_t}{dt^2} + \omega_{Ceo} \frac{d\delta p_t}{dt} + \omega_{eR}^2 \delta p_t = -\tau_t \omega_{Cer} \frac{dp_r}{dt} - \omega_{ei}^2 p_r. \tag{99}$$

The treatment in this paper could be completely formulated in terms of the characteristic frequencies, but the relations are easier to recognize if they are expressed in terms of the conductances C_r and C_o, the masses M_i and M_R, etc. which makes the paper easier to read.

References

[1] S. Backhaus, G.W. Swift, A thermoacoustic-Stirling heat engine: detailed study, *Journal of the Acoustical Society of America* 107 (2000) 3148–3166.
[2] A.T.A.M. de Waele, Regenerator dynamics in the harmonic approximation II, *Cryogenics* 41 (2001) 195–200.
[3] D. Gedeon, Sage: object orientated software for Stirling-type machine design, *Proceedings of the 29th Intersociety Energy Conversion and Engineering Conference*, Vol. 4, American Institute for Aeronautics and Astonautics, Monterey, CA, 1994, pp. 1902–1907.
[4] J. Gary, A. O'Gallagher, R. Radebaugh, E. Marquardt, REGEN3.2 regenerator model: user manual, NIST Technical Note, 2001.
[5] G.W. Swift, *A Unifying Perspective for Some Engines and Refrigerators*, The Acoustical Society of America, 2002 ISBN 0-7354-0065-2.
[6] E. Kreyszig, *Advanced Engineering Mathematics*, Wiley, New York, 1988, p. 443, ISBN 0-471-85824-2.
[7] E. Kreyszig, *Advanced Engineering Mathematics*, Wiley, New York, 1988, p. 117, ISBN 0-471-85824-2.
[8] M. Abramowitz, I.A. Stegun, *Handbook of Mathematical Functions*, Dover Publications, Inc., New York, ISBN 486-61272-4.
[9] J.C.H. Zeegers, M.E.H. Tijani, Personal Communication, 2008.
[10] G. Penelet, V. Gusev, P. Lotton, M. Bruneau, Nontrivial influence of acoustic streaming on the efficiency of annular thermoacoustic prime movers, *Physics Letters A* 351 (2006) 268–273.
[11] G.Y. Yu, E.C. Luo, W. Dai, J.Y. Hu, Study of nonlinear processes of a large experimental thermoacoustic-Stirling heat engine by using computational fluid dynamics, *Journal of Applied Physics* 102 (2007) 074901-1–074901-7.